JOURNAL OF MATERIALS SCIENCE 31 (1996) 4025–4032

Microstructure and composition of Al–Al_2O_3 composites made by reactive metal penetration

Y. GAO*, J. JIA
Department of Materials Engineering, New Mexico Institute of Mining and Technology, Socorro, NM 87801 USA

R. E. LOEHMAN, K. G. EWSUK,
Sandia National Laboratories, Albuquerque, NM 87185 USA

W. G. FAHRENHOLTZ
University of New Mexico, Albuquerque, NM 87106 USA

The microstructure of Al–Al_2O_3 composites made by reactive penetration of Al (or Al alloy) into ceramic (mullite or kaolin) preforms has been investigated using transmission electron microscopy (TEM). The Al–Al_2O_3 composites were found to contain a mutually-interconnected network of Al and Al_2O_3. No crystallographic orientation was observed between the Al and Al_2O_3 phase. Impurities and pores in the ceramic preforms were found to have a strong effect on the microstructure of the composites. The impurities resulted in formation of small particles in the Al_2O_3 grains of Al–Al_2O_3 composites, whereas the porosity yielded a varied ratio of Al to Al_2O_3 in the composites. The growth rate of the Al–Al_2O_3 composites was found to depend on the microstructure and composition of the ceramic preforms as well as the composition of the reactive metals. Pure aluminium penetrated into a dense mullite faster than into a porous mullite at temperatures below 1200 °C. Addition of Mg to Al reduced the growth rate, whereas a continuous phase of amorphous SiO_2 in the ceramic preforms increased the growth rate.

1. Introduction

Metal–ceramic composites have been receiving significant attention in recent years because of their high strength, good fracture toughness, and because of their tailored electrical and thermal properties through control of their composition and microstructure. Interest in commercial applications of such composites has spawned the development of a variety of techniques for synthesis of the metal–ceramic composites [1–5]. Of these techniques, a novel technology based on the directed oxidation of molten components (Lanxide's DIMOX™ Process) [3, 6–10] has been extensively investigated, primarily due to the low cost, shape and dimensional fidelity, low porosity, and ease of fabrication. This process also offers the ability to produce unreinforced [6], particulate-reinforced [3], and fibre-reinforced [11] composites with a wide range of compositions and microstructures. For example, the reaction of a molten aluminium with air produces an Al–Al_2O_3 composite, in which both Al and Al_2O_3 form three-dimensional, interconnected networks [3,6–10]. The reaction product may also be formed as the matrix of a reinforced composite if reinforced particles or fibres are held together in a preform above the molten aluminium.

Recently, a new method for the synthesis of metal–ceramic composites by penetration of a reactive metal into a dense ceramic preform has been reported by Loehman *et al.* [12]. For instance, molten aluminium can penetrate mullite ($Al_6Si_2O_{13}$) at temperatures above 900 °C and convert it to an Al–Si–Al_2O_3 composite based on the oxidation-reduction reaction:

$$3Al_6Si_2O_{13} + (8 + x)Al \rightarrow 13Al_2O_3 + 6Si + xAl \quad (1)$$

where the Gibbs free energy for the reaction is negative, indicating that the reaction is strongly favoured thermodynamically. The principal criteria for successful penetration are a negative Gibbs free energy for the reaction and a favourable wetting of the ceramic by the molten metal. Reactive metal penetration may also be applied to other metal oxide–metal systems as long as the two criteria are satisfied. Recently, we have characterized the microstructure of Al–Al_2O_3 composites made by penetration of molten Al into dense

*Corresponding author. Present address: Pacific Northwest National Laboratory, P.O. Box 999, MS K2-12, Richland, WA 99352, USA

0022–2461

mullite ceramics using transmission electron microscopy [13]. The result showed that the Al–Al_2O_3 composites comprise mutually-interconnected networks of Al and Al_2O_3, similar to that observed in the unreinforced Al–Al_2O_3 composites made by the Lanxide™ process [9,10]. The most important result of the previous investigation was understanding of the formation of the Al–Al_2O_3 composites in the reactive metal penetration process. The formation of the composites proceeds through three stages. Initially, Al penetrates into a dense mullite preform through grain boundary diffusion, and reacts with mullite at grain boundaries to form a partial reaction zone. Then, a complete reaction takes place in the reaction region between the partial reaction zone and the full reaction zone to convert the dense mullite preform to a composite of α-Al_2O_3 (matrix) and an Al–Si phase (thin channels). Finally, the reduced Si from the reaction diffuses out of the Al–Al_2O_3 composite through the metal channels, whereas Al from the molten Al pool is continuously drawn to the reaction region by capillary forces until the mullite preform is consumed or the sample is removed from the molten Al pool. Based on the TEM observations, it was suggested that the penetration kinetics were initially controlled by grain boundary diffusion, but limited by the reaction kinetics at longer penetration times.

The purpose of this paper is to report the results of a similar study of Al–Al_2O_3 composites fabricated by reaction of molten Al or Al alloy with mullite and kaolin preforms. The primary emphasis is to understand the effects of the microstructure and composition of the ceramics, impurities and secondary phases in the ceramics, and alloying elements on the microstructure of the Al–Al_2O_3 composites.

2. Experimental procedure

Reactive metal penetration, which converts ceramic preforms to metal–ceramic composites by direct reduction–oxidation reaction with molten metal, was carried out under an atmosphere of Ti-gettered Ar at temperatures higher than 900 °C. Two types of experiments were employed in the present study. (1) Ceramic preforms (plate, rod, or tube) were dipped in molten aluminium (99.99%) or 6061 aluminium alloy contained in high-purity Al_2O_3 crucibles in a furnace. The temperature of the ceramic preforms was raised rapidly ($dT/dt > 100\,°C\,min^{-1}$) to the processing temperature of 1100–1200 °C. Reaction times of 30 min to 4 h were accurately controlled by dipping the ceramic preforms into molten aluminium for a prescribed time, and then removing it. (2) Composites were prepared directly in a sessile drop apparatus as a by-product of the wetting studies. The ceramic preforms were heated at $20\,°C\,min^{-1}$ to the desired value of 1200 °C and held for up to 8 h while contact angles were measured. After reaction, samples were cooled at $20\,°C\,min^{-1}$ to 700 °C, $5\,°C\,min^{-1}$ from 700–575 °C, and $20\,°C\,min^{-1}$ below 575 °C, respectively. This temperature profile was employed to minimize build-up of stresses during solidification of the metal. Several types of ceramic preforms were used in these experiments, including phase-pure mullite, commercial mullite with a SiO_2-based amorphous phase (MV30, McDanel), porous mullite, and cast kaolin. Details of the composite processing, wetting behaviour, and mechanical properties of the Al_2O_3–Al–Si composites have been reported elsewhere [12].

The microstructure of the representative composites was characterized by transmission electron microscopy (TEM). To prepare TEM specimens, thin slices, 0.5 mm thick, were cut from the bulk samples with a low-speed diamond saw. Specimens of about 3 mm in diameter were then cut from the thin slices of the ceramic preforms and the resultant composites with a coring tool. The specimens were mechanically polished to a nominal thickness of 100 μm, and then dimpled to a thickness of about 15 μm at the centre. Specimens suitable for TEM were finally obtained by ion-beam thinning at liquid-nitrogen temperature. Non-conducting ceramic samples were carbon coated to eliminate charging during the TEM observations. The specimens were examined either in a Philips 420 electron microscope equipped with thin-window energy dispersive spectroscopy (EDX) system operating at 120 keV, or in a Jeol 2000FX transmission electron microscope equipped with a regular EDX system operating at 200 keV.

3. Results and discussion

3.1. An Al–Al_2O_3 composite made from pure Al and phase-pure mullite

Fig. 1a shows a typical TEM image of the microstructure of the phase-pure, dense mullite preforms ($1.27 \times 2.54 \times 5$ cm) used in this experiment. The average grain size was estimated as about 1 μm. The grains are quite uniform, and their boundaries are free of any visible grain–boundary phases. EDX analyses of more than 20 grains indicated that the mullite preform is free of any secondary phases, and that the average atomic ratio of Al to Si is 3 ± 0.05, in agreement with the value of mullite. A representative EDX pattern is shown in Fig. 1b. The mullite phase was further confirmed by electron diffraction patterns (see the inset in Fig. 1a). There are apparently some pores in the mullite preform as shown in Fig. 1a (white regions). However, large thin areas associated with the holes suggest that the holes were likely formed by ion-milling due to their preferred ion-milling rate.

Al–Al_2O_3 composites were formed by dipping the phase-pure, dense mullite preforms in molten aluminium at 1100 °C for a range of times. The growth rate of the composites appears proportional to the square root of time for short times (<1 h), and increases linearly with time afterward at about $3\,mm\,h^{-1}$. The results suggest that there may exist two kinds of growth kinetics, which have been discussed in detail in the previous study [13]. The microstructure of the composites consists of mutually-interconnected Al and Al_2O_3 networks. Fig. 2a shows a typical microstructure of the composite, where the dark grains are alumina and the light grains are aluminium. EDX patterns of aluminium and alumina are shown in Fig. 2(b and c) respectively. A selected-area diffraction

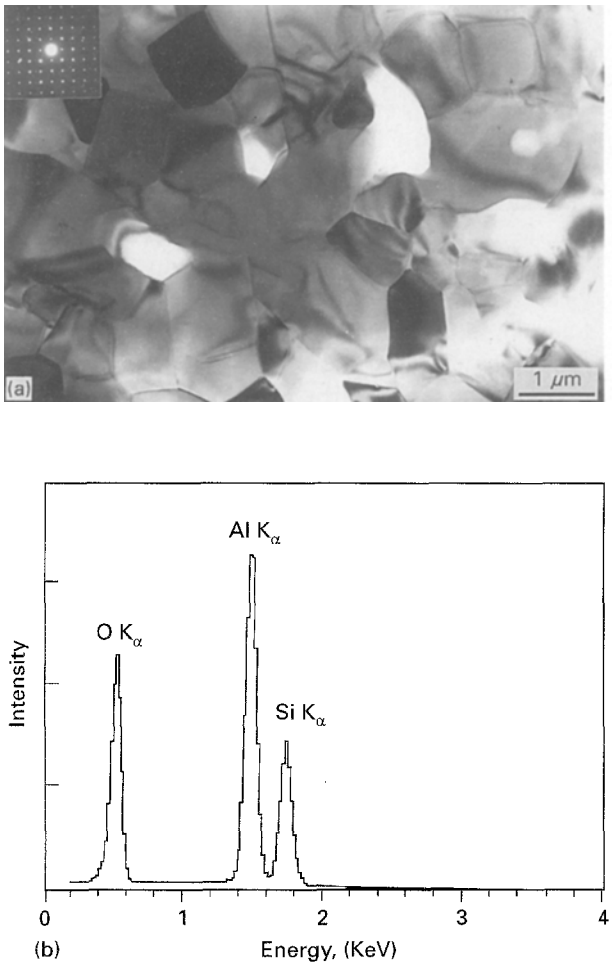

Figure 1 (a) Bright-field TEM image of a phase-pure mullite preform, and (b) a EDX pattern of the mullite phase. An [0 0 1] selected-area electron diffraction pattern of the mullite phase is shown in the inset of (a).

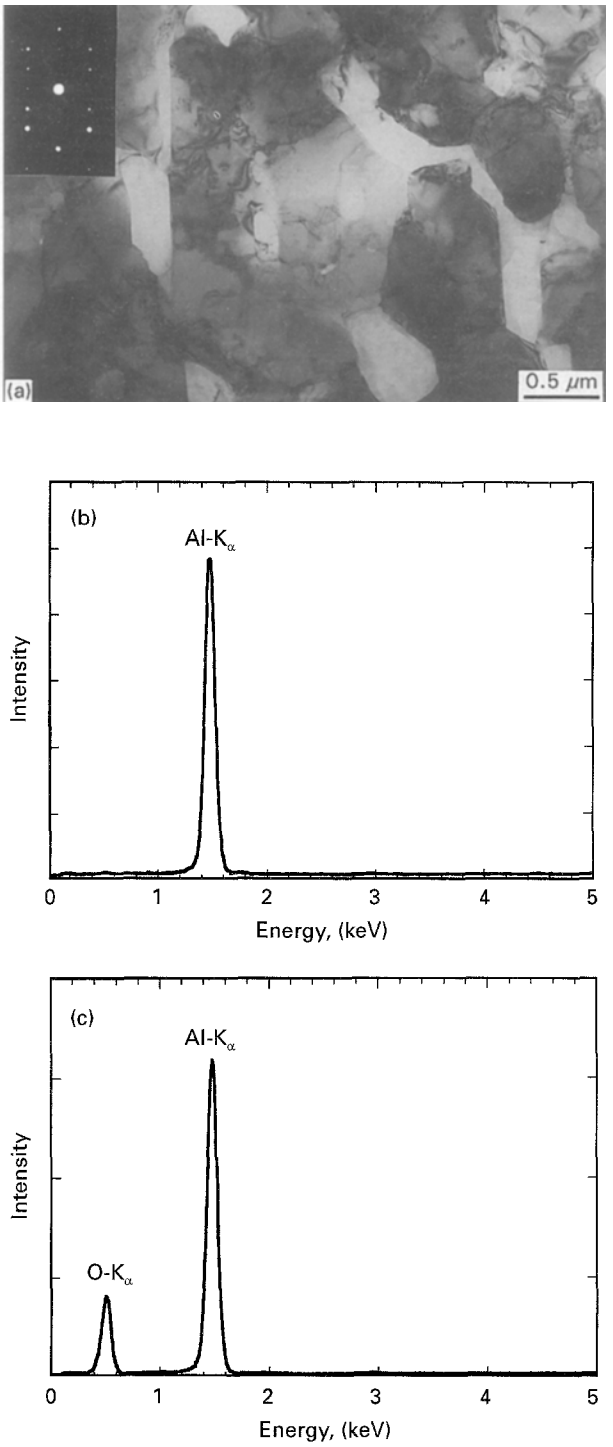

Figure 2 (a) Bright-field TEM image of the Al–Al_2O_3 composites (Al appears light and Al_2O_3 dark) shows a mutually-interconnected network of Al and Al_2O_3. The alumina phase is confirmed as α-Al_2O_3 from a [1 1 $\bar{2}$ 0] selected-area diffraction pattern in the inset. (b) EDX patterns of the Al and (c) EDX pattern of the Al_2O_3.

pattern from an alumina grain in a [11$\bar{2}$0] orientation, shown in the inset of Fig. 2a, indicates that the alumina is α-Al_2O_3. Most of the Al and Al_2O_3 grains show strong faceting with a hexagonal geometry. However, there is no crystallographic orientation relationship found between the Al and α-Al_2O_3 grains from selected-area diffraction patterns of the interfacial areas. It is believed that the faceted shape of the Al grains was not due to their nucleation and growth, but due to the shape of the α-Al_2O_3 grains since the Al grains were still in the liquid state at 1100 °C. The previous study [13] revealed that the geometric shape of the Al and α-Al_2O_3 grains changes from an irregular shape near mullite to a strongly faceted shape at a distance of about 100 μm from the mullite. This indicates that the faceted shape of the α-Al_2O_3 grains is due to the fact that alumina has preferred growth directions (or low-energy surfaces). Such faceted grains were also observed in the Al–Al_2O_3 composites made by the Lanxide™ process [9,14]. The long facets of the Al_2O_3 grains in Fig. 2a were identified as (0001) planes from selected area diffraction patterns. The average grain size of the α-Al_2O_3 was about 2 μm, larger than that of the original mullite. The Al grains appear unconnected with each other in the two-dimensional image (Fig. 2a). However, the composite is a good electrical conductor, indicating that the Al grains are interconnected in three dimension. Therefore, the Al–Al_2O_3 composites fabricated by reactive metal penetration consist of a mutually-interconnected microstructure of Al and α-Al_2O_3, which is similar to the microstructure of unreinforced Al–Al_2O_3 composites produced by the Lanxide™ process [9].

One of the salient features of the Al–Al_2O_3 composites is that the reduced Si from the reaction (see Equation 1) appears missing in the composite. The previous study [13] revealed that the reduced Si diffused out of the composite through the liquid Al

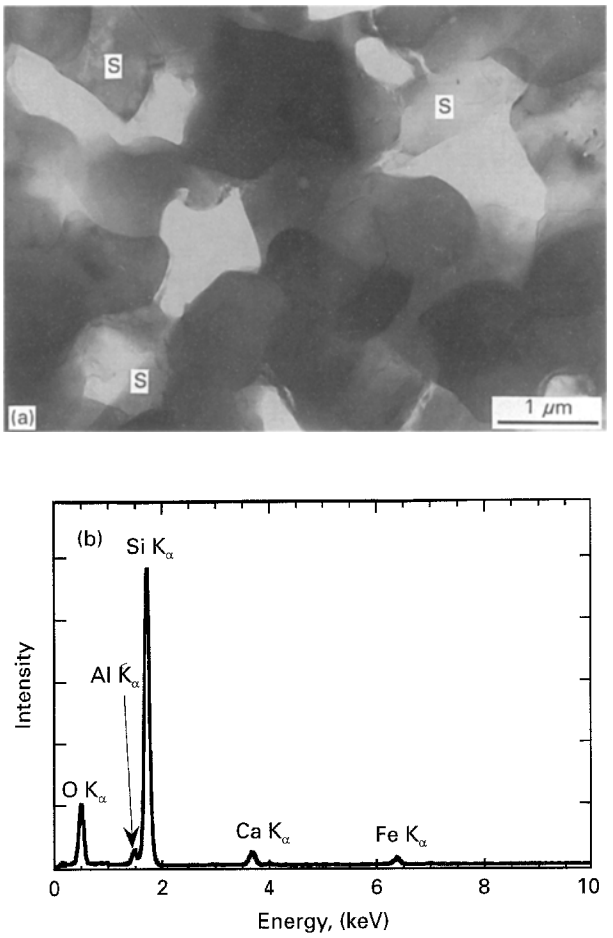

Figure 3 (a) Bright-field TEM image of a commercial mullite tube where amorphous phase marked by S was found from electron diffraction patterns. (b) EDX pattern of the amorphous phase shows that it is amorphous SiO_2 with trace amounts of impurities.

channels during the penetration process, and then dissolved in the molten Al pool used in the dipping experiments. The outward diffusion of the reduced Si strongly affects the penetration kinetics. One may also note that the phenomenon of removing Si from the composites is similar to zone refining.

3.2. The effect of impurities and secondary phases in mullite on the formation of an Al–Al_2O_3 composite

In order to understand the effects of impurities and secondary phases in mullite on the formation of the Al–Al_2O_3 composites, a penetration experiment was carried out using a commercial mullite tube (1.8 cm OD, 1.2 cm ID, and 5 cm long) with a SiO_2-based glassy phase as the ceramic preform. The mullite tube was reacted by placing Al on the inside. The tube was then heated to 1200 °C in a horizontal configuration, the Al melted and formed a pool in the bottom all along the tube length. As progress is made up the side of the tube towards the top, one is moving away from the point of origin of the reaction. Fig. 3a shows a typical TEM image of the mullite tube. The average grain size was estimated to be about 1 μm, similar to that of the phase-pure mullite preform (Fig. 1a). EDX results of more than 20 grains indicated that about 80% of the grains are mullite, whereas about 15% of the grains are SiO_2 as marked by the letter S in Fig. 3a. Almost all of the SiO_2 grains contain trace amounts of impurities such as Fe, K, Ca or Ti as well as Al. A representative EDX pattern of the SiO_2 phase is shown in Fig. 3b. Selected area diffraction patterns from the SiO_2 grains showed an amorphous-like ring pattern, indicating that the SiO_2 phase is amorphous. Pores of about 5% are also apparent in Fig. 3a.

The microstructure of the composite tube varies along the tube circumference since a part of the tube was in contact with the molten Al. The microstructure at the bottom part of the composite tube is similar to that in Fig. 2a, consisting of Al and Al_2O_3 mutually-interconnected networks. However, there exist two major differences between the microstructures of the two composites. Firstly, the average grain size of the α-Al_2O_3 grains is about 4 μm, larger than the grain size of about 2 μm in Fig. 2a, while the size of the Al grains has a bi-size distribution: ~0.5 μm and ~1.0 μm. The large Al grains were probably formed in a different way from the small ones which were formed during the reaction [13]. The large Al grains could be simply formed by filling the pores in the mullite tube with Al during penetration. The growth rate of the composite is similar to that of the composites made from the phase-pure, dense mullite. However, the penetration rate of Al into a SiO_2 glass reported by Prabriputaloong and Piggott [15] is much higher than the growth rate observed in the present study. They found that the thickness of the reacted layer reached 0.5 mm after dipping a SiO_2 glass rod in Al at 800 °C for only 5 min, compared to the growth rate of 3.5 mm h^{-1} for penetration of Al into a dense, phase-pure mullite preform. Thus, one would expect a higher growth rate of the composites in this system since the mullite tube consists of ~15% amorphous SiO_2. It is believed that the growth rate was not increased because the SiO_2 glassy phase was not connected to each other to form a continuous path in the mullite tube. An increase in the growth rate has indeed been observed in the Al-cast kaolin system, where a continuous matrix of amorphous SiO_2 was observed in the cast kaolin preform (see Section 3.4).

Secondly, a variety of particles were observed in the α–Al_2O_3 grains of the composite. A typical TEM image of such particles is shown in Fig. 4a. The size of the particles varies from 20 nm to 0.4 μm in diameter, and the composition of the particles changes from Si-rich to Al-rich. In general, large particles (≥0.1 μm) are Si-rich whereas small particles (≤50 nm) are Al-rich. Typical EDX patterns of a Si-rich particle and an Al-rich one are shown in Fig. 4(b and c) respectively. The Al concentration in the small particles could have been enhanced by a relative large electron beam size (50 nm) used in collecting the EDX patterns. The impurities observed in the SiO_2 amorphous phase of the mullite tube were found in the particles. In addition, most of the particles showed the same kind of faceting as observed for the Al grains in the composite. However, no crystallographic orientation relationship was found between the particles and the α–Al_2O_3 matrix, indicating that the particles are not precipitates.

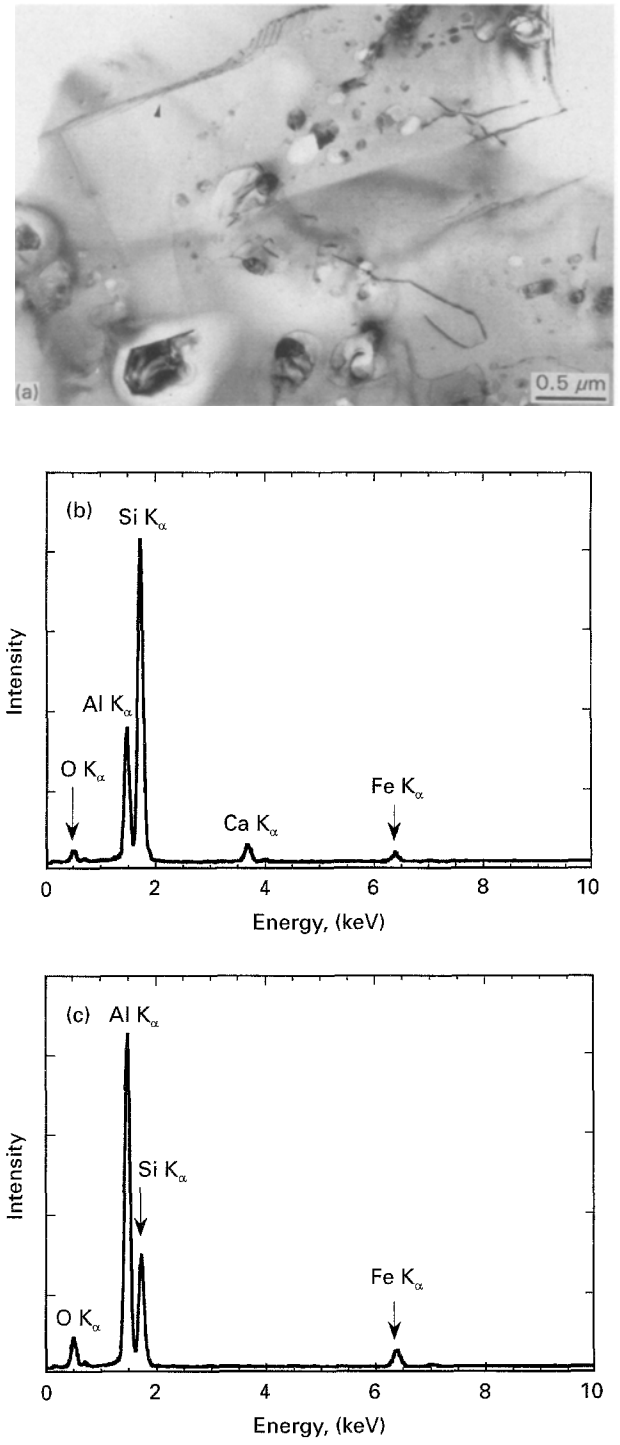

Figure 4 (a) TEM image shows a variety of particles in an Al_2O_3 grains of the composite. A low-angle boundary is indicated by an arrow. EDX patterns of a large particle and a small one are shown in (b) and (c), respectively. Impurities are found in most of the particles.

It is believed that they were liquid at the penetration temperature, and were trapped inside the α–Al_2O_3 matrix during the formation of the α–Al_2O_3 from mullite. Therefore, the formation of the particles is likely a result of local accumulation of the impurities during the reaction since the impurities could not be consumed in the reaction of Al with mullite.

In contrast to the bottom part of the tube, the top part of the tube (which was above the surface of the molten Al) was not directly in contact with molten Al. As a result, the composite has different constituents

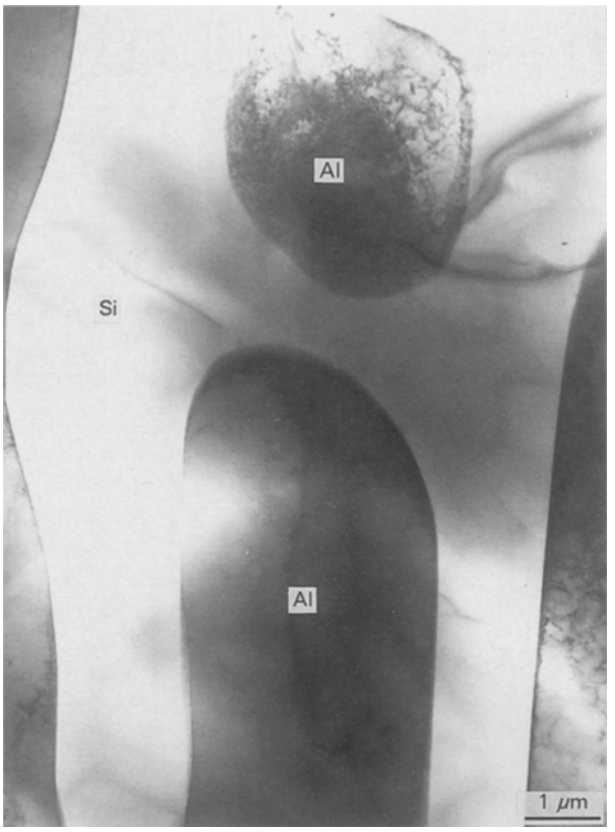

Figure 5 Eutectic structure of Si and Al observed in the remaining Al at room temperature.

(Al, Al_2O_3, and Si), and its microstructure consists of an interconnected network of Al, Si, and Al_2O_3. The percentage of Al plus Si is similar to that of Al in the composite at the bottom part. However, the ratio of Al to Si in the composite varies from $\sim$100% at the bottom part of the composite tube to $\sim$20% near the top of the tube, which is expected since removal of the reduced Si from the composite was controlled by a diffusion process. TEM and optical microscopy of the remaining Al showed that the remaining Al at room temperature consists of large Si crystals and an eutectic structure of Al and Si (see Fig. 5). This indicates that the concentration of Si in the remaining Al at the processing temperature was higher than 12.2 at% (the eutectic composition) [16]. The high concentration of Si in the remaining Al plus the long diffusion path could largely slow down the outward diffusion of Si from the top part of the tube. As a result, most of the reduced Si was retained in the composite after the processing. This is consistent with the observation of the eutectic structure of Al and Si in the composite near the top of the tube. Fig. 6 shows an example of the eutectic structure in the composite, where a Si grain is found adjoining to an Al grain. Dislocations are clearly visible in the Al grain, whereas twins, marked by the letter T, are found in the Si grain. Note that the diffraction condition used in Fig. 6 was chosen to show the best contrast for the dislocations, but not for the twin boundaries. Formation of the defects was to accommodate the deformation induced by the thermal stress during cooling down to room temperature. The thermal stress is due to a large thermal mismatch among Al_2O_3, Al, and Si.

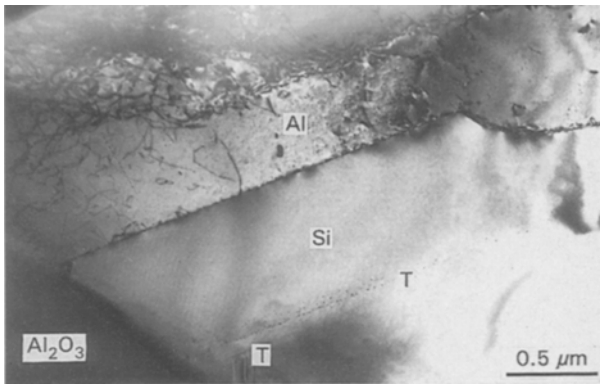

Figure 6 A silicon grain is observed adjoining to an aluminium grain in the composite close to the top of the composite tube. Dislocations and twins (T) are seen in Al and Si, respectively.

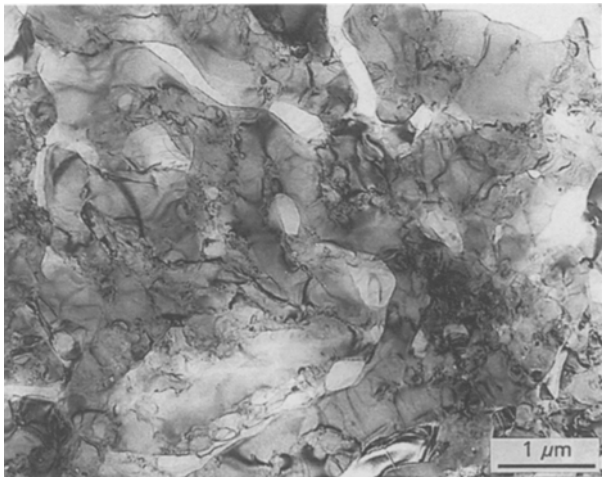

Figure 7 Microstructure of the Al–Al_2O_3 composite (Al appears light and Al_2O_3 dark) made by penetration of 6061 Al alloy into a dense mullite preform.

3.3. The effect of the Al alloy on the formation of an Al–Al_2O_3 composite

Pure Al was replaced by 6061 Al alloy (alloying elements being Mg, Si, Mn etc.) to study the effect of alloying elements on the formation of the Al–Al_2O_3 composite. The experiment was carried out by dipping a phase-pure mullite rod (2.5 cm in diameter) in molten Al alloy at 1100 °C for 30 min. The growth rate of the composite was found to be much slower than that in the pure Al-mullite system. After 30 min reaction, only a thin composite layer of about 0.2 mm thickness was formed. Fig. 7 shows a typical TEM image of the microstructure of the resultant composite. The overall microstructure is similar to that observed in the pure Al–mullite system (Fig. 2a). However, the shape of the Al_2O_3 and Al grains is irregular as observed in the composite near mullite in the pure Al–mullite system [13]. This indicates that the reaction is inhibited by the presence of Mg in the Al alloy. In addition, the composite consists of a notable amount of Si grains. The alloying elements such as Mg were found in the Al_2O_3, Al, and Si grains. However, their oxides were not observed in the composite.

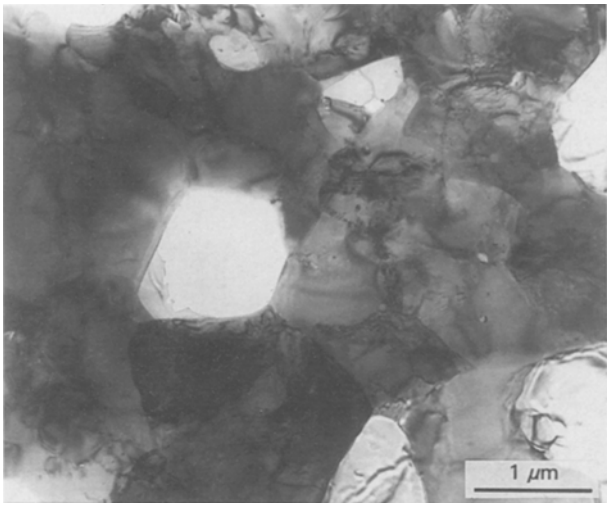

Figure 8 Microstructure of the Al–Al_2O_3 composite (Al appears light and Al_2O_3 dark) made by penetration of Al into a porous mullite preform.

The present observations are different from the results reported by Antolin *et al.* for the Al–Al_2O_3 composite made by the Lanxide™ process [10]. They found that the addition of Mg to Al significantly enhanced the formation of the composites. It was believed that the addition of Mg could reduce the surface tension of molten Al and hence improve the wetting of the reaction product (Al_2O_3) by the Al alloy. They concluded that the addition of Mg to Al is essential for the Lanxide™ process since the formation of a thin MgO layer on the surface permits the development of the dissolution–precipitation process (growth mechanism) and prevents the formation of a protective layer of Al_2O_3 on the surface. However, the growth rate of the Al–Al_2O_3 composites in the present study was slower when Al was replaced by the 6061 Al alloy. Thus, we believe that the addition of Mg to Al must play an opposite role in reactive metal penetration, which is not impossible since the growth mechanism of the composites by the two processing techniques are completely different [10, 13]. It is postulated that a thin layer of MgO similar to that observed in the Lanxide™ process could be formed at the interface between molten Al alloy and mullite. However, the MgO layer prohibits Al penetrating into, and Si diffusing out of, the composite resulting in a low growth rate for the composite. This is also consistent with the observation of retained Si grains in the composite.

3.4. The effect of the porosity in mullite on the formation of an Al–Al_2O_3 composite

The penetration of Al into a porous mullite was performed by the sessile drop method to study the effect of the porosity on the formation of the composite. It was found that Al penetration into the porous mullite is slower than its penetration into dense mullite ceramics at temperatures below 1200 °C. Fig. 8 shows a typical TEM image of the microstructure of the composite. In contrast to the small, long,

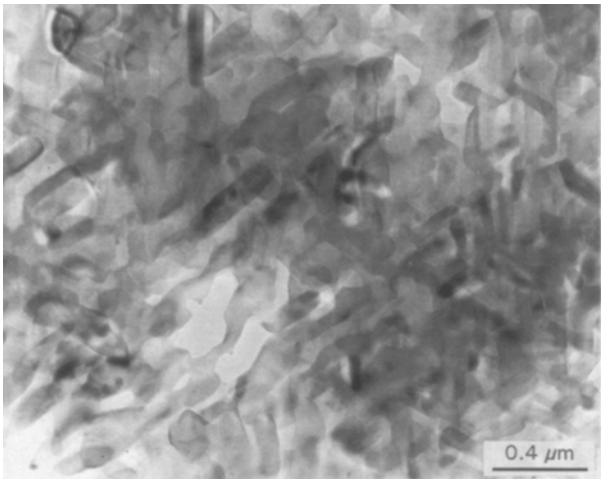

Figure 9 TEM image of the cast kaolin preform showing that small kaolin crystals are dispersed in a continuous amorphous phase of SiO_2.

connected Al grains in Fig. 2a, a majority of the Al grains in the composite are large and isolated. More than 35% of the composite is Al, compared to less than 25% in the composites made from the dense mullite ceramics. The large Al grains are clearly due to the existence of the pores in the porous mullite. It is believed that a large portion of the penetrated Al filled the pores, rather than reacting with the mullite to produce Al_2O_3 and Si, leading to a low growth rate for the composite. This composite is a poor electrical conductor with a resistivity of about 1000 Ω-cm, which is the result of the poor percolation path of the Al grains in the composite. Thus, the Al–Al_2O_3 composite is an Al_2O_3-matrix composite with poorly-connected Al grains. The results clearly show that the microstructure and composition of the Al–Al_2O_3 composites can be easily tailored by selecting different microstructure of the mullite preforms.

3.5. The effect of the starting ceramics on the formation of an Al–Al_2O_3 composite

The Al–mullite system has been explored as a model system for reactive metal penetration to synthesize Al–Al_2O_3 composites. This technique has also been successfully extended to other systems such as Al–kaolin ($Al_2Si_2O_5(OH)_4$) for fabrication of Al–Al_2O_3 composites. In this case, kaolin preforms were prepared by casting. The cast kaolin preforms were very porous, and large pores were clearly visible on the surface. Fig. 9 shows a TEM image of the cast kaolin, where small kaolin crystals ($\sim 0.1 \times 0.3$ μm) are dispersed in a continuous matrix. The microstructure is apparently different from those of the mullite ceramics. The structure of the kaolin crystals was confirmed from high-resolution TEM images and micro electron diffraction patterns. Furthermore, the atomic ratio of Al to Si was found to be 1 ± 0.1 from EDX patterns of more than 10 kaolin crystals, which is in agreement with the value of kaolin. The matrix was identified as amorphous SiO_2 from EDX and selected-area electron diffraction.

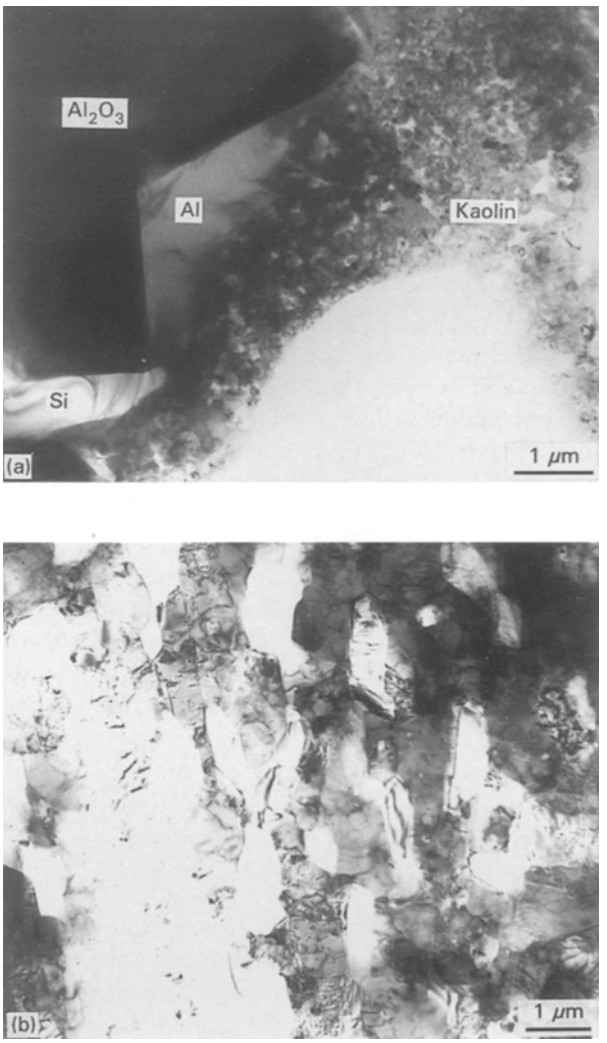

Figure 10 (a) TEM image showing the transition layer between the kaolin preform and composite, where the unreacted kaolin, reaction products (Si and Al_2O_3), and Al are found. (b) Microstructure of the Al–Al_2O_3 composite (Al appears light and Al_2O_3 dark) made by penetration of Al into a cast kaolin preform.

The composite was fabricated by the sessile drop experiment at 1200 °C for 8 h. Reactive penetration of Al into the cast kaolin preform was stopped before the completion of the reaction. As a result, a part of the kaolin preform remained unreacted. A thin intermediate layer (light brown) of about 0.2 mm thickness was clearly visible under an optical microscope between the composite (dark) and the kaolin (white). The thin layer is very similar to the partial reaction zone observed in the Al–mullite system [13]. The TEM image of the layer in Fig. 10a clearly shows that the intermediate layer consists of unreacted kaolin crystals, the reaction products (Al_2O_3 and Si) as well as penetrated Al. This indicates that the intermediate layer is a transition region from the kaolin to the composite. Furthermore, the microstructure of the Al_2O_3, Si, and Al phases is similar to that observed in the partial reaction zone of the Al–mullite system although the microstructure and composition of the starting ceramics are completely different. Observation of the transition layer suggests that the penetration process in the Al–kaolin system is controlled by the reaction kinetics, similar to that in the Al–mullite system [13].

Fig. 10b shows the microstructure of the composite, which is similar to that observed in Fig. 2a for the Al–mullite system. The composite consists of mutually-interconnected Al (light phase) and α-Al_2O_3 (dark phase) networks. It appears that both Al and Al_2O_3 grains are aligned, or elongated in the penetration direction (from top to bottom in Fig. 10b). A similar alignment was also observed in the Al–mullite systems, as shown in Fig. 2a. The similarity of the final microstructures of the Al–Al_2O_3 composites further confirms the similar penetration kinetics for the two systems. However, the growth rate of the composite in the Al–kaolin system was found to be higher than that in the Al–mullite system. The higher growth rate could simply be a result of a faster reaction of Al with kaolin (compared to Al with mullite), or the smaller size of the kaolin crystals (compared to the mullite grains), or a combination of both. In the first case, the faster reaction between Al and kaolin, together with the faster reaction between Al and amorphous SiO_2 [15], will result in a higher growth rate for the composite. In the second case, the smaller size of the kaolin crystals requires a shorter time for a complete reaction for each kaolin crystal with Al, leading to a higher growth rate for the composite.

4. Summary

The present results clearly show that the new route for synthesis of Al–Al_2O_3 composites by reactive penetration of Al (or Al alloy) into a dense ceramic preform (mullite or kaolin) offers the ability to produce metal–ceramic composites with a wide range of compositions and microstructures. Microstructurally, all of the Al–Al_2O_3 composites were found to consist of mutually-interconnected Al (Si) and Al_2O_3 networks, regardless of the composition and microstructure of the ceramic preforms. No crystallographic orientation was observed between the Al and Al_2O_3 phase, and between the Al_2O_3 grains. Other microstructural features of the composites including grain size, small particles, and the ratio of Al (Si) to Al_2O_3 were largely controlled by the microstructures of the ceramic (mullite or kaolin) preforms (grain size, porosity, impurities, composition, secondary phases, etc.). Impurities in the ceramic preforms resulted in the formation of small particles in the Al_2O_3 grains of the Al–Al_2O_3 composites, whereas the porosity and SiO_2-based amorphous phase in the ceramic preforms yielded a varied ratio of Al (Si) to Al_2O_3 in the composites.

The growth rate of the Al–Al_2O_3 composites (or penetration rate) was found to depend on the microstructure and composition of the ceramic preforms as well as the composition of the reactive metals. Pure aluminium penetrated into a dense mullite faster than into a porous mullite at temperatures below 1200 °C. The addition of Mg to Al reduced its penetration capability, whereas a continuous matrix of amorphous SiO_2 in ceramic preforms increased the growth rate.

Acknowledgements

This work was supported by the U.S. Department of Energy under contract No. DE–AC04–76DP00789 at Sandia National Laboratories. The use of the Jeol 2000FX transmission electron microscope in the Department of Geology, University of New Mexico, is gratefully acknowledged.

References

1. M. J. KOCZAK and M. K. PREMKUMAR, *J. of Metals* **45** (1993) 44.
2. V. V. KRSTIC, P. S. NICHOLSON and R. G. HOAGLAND, *J. Amer. Ceram. Soc.* **64** (1981) 499.
3. M. S. NEWKIRK, H. D. LESHER, D. R. WHITE, C. R. KENNEDY, A. W. URQUHART and T. D. CLAAR, *Ceram. Eng. Sci. Proc.* **8** (1987) 879.
4. F. F. LANGE, B. V. VELAMAKANNI and A. G. EVANS, *J. Amer. Ceram. Soc.* **73** (1990) 388.
5. T. D. CLAAR, W. B. JOHNSON, C. A. ABDERSSON and G. H. SCHIROKY, *Ceram. Eng. Sci. Proc.* **10** (1989) 599.
6. M. S. NEWKIRK, A. W. URQUHART and H. R. ZWICKER, *J. Mater. Res.* **1** (1986) 81.
7. M. K. AGHAJANIAN, N. H. MACMILLAN, C. R. KENNEDY, S. J. LUSZCZ and R. ROY, *J. Mater. Sci.* **24** (1989) 658.
8. M. K. AGHAJANIAN, M. A. ROCAZELLA, J. T. BURKE and S. D. KECK, *ibid.* **29** (1991) 447.
9. E. BREVAL, M. K. AGHAJANIAN and S. J. LUSZCZ, *J. Amer. Ceram. Soc.* **73** (1990) 2610.
10. S. ANTOLIN, A. S. NAGELBERG and D. K. CREBER, *ibid.* **75** (1992) 447.
11. A. S. FAREED, B. SONUPARLAK, C. T. LEE, A. J. FORTINI and G. H. SCHIROKY, *Ceram. Eng. Sci. Proc.* **11** (1990) 782.
12. R. E. LOEHMAN, K. EWSUK and A. P. TOMSIA, *J. Amer. Ceram. Soc.* **79** (1996) 27.
13. Y. GAO, J. JIA, R. E. LOEHMAN and K. G. EWSUK, *J. Mater. Res.* **10** (1995) 1216.
14. B. D. FLINN, M. RUHLE and A. G. EVANS, *Acta Metall. Mater.* **37** (1989) 3001.
15. K. PRABRIPUTALOONG and M. R. PIGGOTT, *J. Amer. Ceram. Soc.* **58** (1975) 184.
16. T. B. MASSALSKI, "Binary alloy phase diagrams" 2nd Edn (ASM International, Materials Park, OH, 1990)

Received 5 July 1995
and accepted 21 December 1995